

# Getting topological invariants from snapshots: a protocol for defining and calculating topological invariants of systems with discrete parameter space

Youjiang Xu, Walter Hofstetter

Goethe-Universität, Institut für Theoretische Physik, 60438 Frankfurt am Main, Germany

Topological invariants, including the Chern numbers, can topologically classify parameterized Hamiltonians. We find that topological invariants can be properly defined and calculated even if the parameter space is discrete, which is done by geodesic interpolation in the classifying space. We specifically present the interpolation protocol for the Chern numbers, which can be directly generalized to other topological invariants. The protocol generates a highly efficient algorithm for numerical calculation of the second and higher Chern numbers, by which arbitrary precision can be achieved given the values of the parameterized Hamiltonians on a coarse grid with a fixed resolution in the parameter space. Our findings also open up opportunities to study topology in finite-size systems where the parameter space can be naturally discrete.

Topological invariants can indicate whether it is possible to continuously deform two manifolds into each other [1]. They appear in various systems, classifying parameterized Hamiltonians or their eigenstates [2–10]. For example, it is well known that in the Integer Quantum Hall Effect, the Hall conductivity can only take integer values because it is proportional to the 1st Chern number, a topological invariant characterizing how the two-dimensional Brillouin zone is mapped to single-particle Hamiltonians in momentum space [11–13]. The integer-valued 2nd and higher Chern numbers can also show up as electromagnetic response [14, 15] or in quasicrystals [16–18]. However, it is challenging to numerically calculate these quantities from the Hamiltonians. This difficulty is illustrated by the following example.

Consider the Chern numbers of the family of single-particle Hamiltonians  $H(\mathbf{k})$  parameterized by a vector  $\mathbf{k} \in K$ , where  $K \equiv [0, 1]^D$  is the  $D$ -dimensional parameter space.  $H(\mathbf{k})$  is an  $s \times s$  hermitian matrix that is periodic in each component  $(k^1, k^2, \dots, k^D)$  of  $\mathbf{k}$  with period 1, and it can also be regarded as a mapping from  $K$  to  $s \times s$  hermitian matrices. Suppose  $H(\mathbf{k})$  describes a fermionic topological insulator gapped at zero energy for all  $\mathbf{k}$ , i.e., the number of negative eigenvalues of  $H(\mathbf{k})$ , denoted as  $r$ , is independent of  $\mathbf{k}$ . We represent the  $r$  lower-energy eigenstates of  $H(\mathbf{k})$  by an  $s \times r$  matrix, denoted as  $V(\mathbf{k})$ , where each column of  $V(\mathbf{k})$  is one of these normalized eigenstates occupied by a fermion.  $V(\mathbf{k})$  satisfies  $V^\dagger(\mathbf{k})V(\mathbf{k}) = 1$ , and the collection of  $s \times r$  matrices satisfying this relation forms the (complex) Stiefel manifold  $\text{St}(s, r) \equiv \frac{U(s)}{U(s-r)}$ , where  $U(\cdot)$  represents the unitary group. Then, the matrix forms of the Berry connection and the Berry curvature are given by  $\mathcal{A}_\mu \equiv V^\dagger \partial_\mu V$  and  $\mathcal{F}_{\mu\nu} = \partial_\mu \mathcal{A}_\nu - \partial_\nu \mathcal{A}_\mu + [\mathcal{A}_\mu, \mathcal{A}_\nu]$ , respectively, where  $\partial_\mu \equiv \frac{\partial}{\partial k^\mu}$ . The  $n$ th Chern character  $\text{ch}_n \equiv \frac{\epsilon^{\mu_1 \lambda_1 \mu_2 \lambda_2 \dots \mu_n \lambda_n}}{n!} \left(\frac{i}{4\pi}\right)^n \text{tr} [\mathcal{F}_{\mu_1 \nu_1} \mathcal{F}_{\mu_2 \nu_2} \dots \mathcal{F}_{\mu_n \nu_n}]$ , where  $\epsilon^{\mu_1 \lambda_1 \mu_2 \lambda_2 \dots \mu_n \lambda_n}$  is the Levi-Civita symbol, is integrated to give the  $n$ th Chern number  $c_n$ , i.e.,  $c_n \equiv \int \text{ch}_n d^{2n}k$ , where the domain of the integral is a certain  $2n$ -dimensional subspace of  $K$ , usually  $K$

itself. Both  $c_n$  and  $\text{ch}_n$  are functionals of  $V$ , so they can be denoted as  $c_n[V]$  and  $\text{ch}_n[V]$ , respectively. Numerically, we may straightforwardly follow these defining expressions to calculate the Chern numbers: First, we discretize the parameter space  $K$  by the grid  $K_0 \equiv \{0, N_0^{-1}, 2N_0^{-1}, \dots, 1\}^D$ , which divides  $K$  into  $N_0$  (integer) segments in each dimension. Then, for any point on the grid,  $\boldsymbol{\kappa} \in K_0$ , we get the Hamiltonian  $H(\boldsymbol{\kappa})$ , diagonalize it to obtain  $V(\boldsymbol{\kappa})$ , from which we approximate  $\mathcal{F}_{\mu\nu}(\boldsymbol{\kappa})$  by finite difference methods, and finally calculate the sum  $\sum_{\boldsymbol{\kappa}} \text{ch}_n(\boldsymbol{\kappa})$  to get  $c_n$ . The precision of such algorithms depends on the grid density  $N_0$ . For example, the authors [19] follow these steps to calculate  $c_2$ , and their algorithm is claimed to be efficient because they found a good way to approximate  $\mathcal{F}_{\mu\nu}(\boldsymbol{\kappa})$  using  $V(\boldsymbol{\kappa})$ . However, the algorithm in [19] still requires a large  $N_0$ , e.g. 60, to reach convergence, i.e. the algorithm requires  $60^4$  Hamiltonians  $H(\boldsymbol{\kappa})$  to be diagonalized, which can be too costly, especially when  $H(\boldsymbol{\kappa})$  are effective topological Hamiltonians [20, 21] that characterizes topology of interacting systems, and obtaining a single  $H(\boldsymbol{\kappa})$  requires a significant amount of computing resources. Another problem of such algorithms is that they cannot efficiently pinpoint the topological phase boundaries where the topological invariant  $c_n$  jumps. This is because near the boundaries,  $\text{ch}_n(\mathbf{k})$  peaks in small regions of  $K$ , and it is very inefficient to capture the peak profile by increasing  $N_0$ .

These problems are avoided in the widely used algorithm calculating  $c_1$  [22]. The authors of [22] show that the exact value of  $c_1$  can be obtained with a fixed small  $N_0$ . In this paper, we show that this is true for any Chern number  $c_n$ , which is achieved by a proper *ab initio* definition of the Chern numbers in a discrete parameter space following a protocol of interpolation. We will use the algorithm arising from this new protocol to calculate  $c_2$  for the lattice Dirac model and show its significant advantages in comparison to the previous algorithm in [19]. Also, our protocol can reproduce and provide an explanation for the existing algorithm for  $c_1$  in [22], and can

be directly generalized to other topological invariants besides Chern numbers.

The basic idea behind the protocol can be illustrated as follows: Consider an object periodically moving around a circle with its trajectory described by the azimuth  $\theta(t)$ , a continuous function of time  $t$  satisfying the periodic boundary condition  $\theta(t+1) = 2\pi w + \theta(t)$ , where the winding number  $w$ , which counts the number of circles the object completes in a period, is the topological invariant that classifies the motion or the mapping  $\theta(t)$ . We can measure  $\theta(t)$  to get  $w$ . In practice, it is impossible to measure  $\theta(t)$  at every moment  $t$ , instead, we measure  $\theta(t_i)$  at a finite number of times  $t_1, t_2, \dots, t_N$ , supposing  $t_N = t_1 + 1$ , so the information at hand is a discrete mapping  $\theta(t_i)$ . Notice that we can determine  $\theta(t_i)$  only up to modulo of  $2\pi$ , because  $\theta$  and  $\theta + 2\pi$  represent the same physical position. If we assume that  $\theta(t_i)$  is measured so frequently that the object never moves more than half a circle between adjacent measurements, we can eliminate the uncertainty of  $\theta(t_{i+1}) - \theta(t_i)$ . For example, if  $\theta(t_1) = 0$  and  $\theta(t_2) = 2\pi m + \delta$  with an unknown integer  $m$  and a small  $\delta$  satisfying  $|\delta| < \pi$ , then  $m$  has to be 0. In this way, we obtain the difference  $\theta(t_N) - \theta(t_1)$  as well as the winding number. For more complicated systems, topological invariants can rarely be obtained from a simple subtraction like this, but from certain defining integrals, e.g., the Chern numbers are integrals of Chern characters. Such a defining integral for  $w$  is  $w = \int_0^1 \frac{dt}{2\pi} \frac{d\theta(t)}{dt}$ . The assumption we made implies that the same winding number can also be obtained from  $w = \int_0^1 \frac{dt}{2\pi} \frac{d\tilde{\theta}(t)}{dt}$ , where  $\tilde{\theta}(t) \equiv \frac{(t_{i+1}-t)\theta(t_i) + (t-t_i)\theta(t_{i+1})}{t_{i+1}-t_i}$  with  $t \in [t_i, t_{i+1}]$  and  $\tilde{\theta}(t)$  is defined for all intervals  $[t_i, t_{i+1}]$  with any  $i$ .  $\tilde{\theta}(t)$  is a continuous function in  $[0, 1]$ , but its derivative  $\frac{d\tilde{\theta}(t)}{dt}$  is discontinuous at  $t = t_i$ , which does not make the integral  $\int_0^1 \frac{dt}{2\pi} \frac{d\tilde{\theta}(t)}{dt}$  ill-defined. Notice that in the interval  $[t_i, t_{i+1}]$ ,  $\tilde{\theta}(t)$  is one of the geodesics that interpolates  $\theta(t_i)$  and  $\theta(t_{i+1})$ , in the sense that the distance between  $\theta(t_i)$  and  $\theta(t_{i+1})$  given by  $\int_{t_i}^{t_{i+1}} |d\tilde{\theta}|$  is its minimum  $|\theta(t_i) - \theta(t_{i+1})|$ . Meanwhile, any function  $\tilde{\theta}(\lambda(t))$ , where  $\lambda(t)$  satisfies  $\lambda(t_i) = t_i$ ,  $\lambda(t_{i+1}) = t_{i+1}$  and  $\frac{d\lambda(t)}{dt} > 0$ , represents the same geodesic, and replacing  $\tilde{\theta}(t)$  by  $\tilde{\theta}(\lambda(t))$  in  $\int_0^1 \frac{dt}{2\pi} \frac{d\tilde{\theta}(t)}{dt}$  does not affect the winding number. This is because  $\tilde{\theta}(t)$  and  $\tilde{\theta}(\lambda(t))$  are homotopic with each other (also with  $\theta(t)$ ), i.e., they can be converted into each other by a continuous deformation. Because the explicit form of  $\theta(t)$  does not affect the winding number calculated from  $\tilde{\theta}(t)$ , we can *ab initio* define the winding number of the discrete mapping  $\theta(t_i)$  by that of its geodesic interpolant  $\tilde{\theta}(t)$ , without  $\theta(t)$  coming into play. We will show that the very idea of geodesic interpolation can also be used to define the Chern numbers in discrete parameter spaces.

The goal is to find a proper definition of the Chern

numbers knowing only the discrete mapping  $H(\boldsymbol{\kappa})$  with  $\boldsymbol{\kappa} \in K_0$ . The definition only makes sense if the Chern numbers of the discrete mapping  $H(\boldsymbol{\kappa})$  coincide with that of the continuous mapping  $H(\mathbf{k})$  given a large enough  $N_0$ . Provided the geodesic interpolants of  $V(\boldsymbol{\kappa})$ , denoted as  $\tilde{V}(\mathbf{k})$ , we define the Chern numbers of the mapping  $H(\boldsymbol{\kappa})$  as  $c_n[\tilde{V}]$ , and we will show how to obtain  $\tilde{V}(\mathbf{k})$  from  $V(\boldsymbol{\kappa})$ .

Now,  $V(\boldsymbol{\kappa})$  plays a similar role as  $\theta(t_i)$  in the previous example. We know  $\theta$  has the uncertainty of modulo of  $2\pi$ , which however does not affect the winding number. A similar situation occurs with any  $V \in \text{St}(s, r)$ . Physically,  $V$  corresponds to a many-body state of  $r$  fermions, the Slater determinant of the  $r$  occupied states. The physical many-body state is invariant under the gauge transformation represented by a  $r \times r$  unitary matrix  $g$ , i.e.,  $V$  and  $Vg$  represent the same physical state, which we denote by  $V \simeq Vg$ . As a result, Chern numbers should not change under gauge transformations, i.e.,  $c_n[V] = c_n[V']$  if  $V(\mathbf{k}) \simeq V'(\mathbf{k})$  for all  $\mathbf{k}$ . So what really matters in determining the topology is the gauge invariant projection operator  $\rho(\mathbf{k}) \equiv V(\mathbf{k})V(\mathbf{k})^\dagger$  that belongs to the (complex) Grassmann manifold,  $\text{Gr}(s, r) \equiv \frac{U(s)}{U(r)U(s-r)}$ , and an element in  $\text{Gr}(s, r)$  can be represented by different elements in  $\text{St}(s, r)$  that are related by gauge transformations. If we regard a single-particle state as a vector in the space  $\mathbb{C}^s$ , then  $\rho(\mathbf{k})$  projects this vector to the hyperplane spanned by column vectors of  $V(\mathbf{k})$ , so  $\rho$  as well as its corresponding many-particle state can be geometrically interpreted as this hyperplane, and  $\text{Gr}(s, r)$  is the collection of such  $r$ -dimensional hyperplanes that contain the origin of  $\mathbb{C}^s$ . This geometric interpretation helps to find the geodesics in  $\text{Gr}(s, r)$ .

With the Riemannian metric, the distance between these hyperplanes is measured by the angles between them [23, 24]. Consider two hyperplanes represented by  $V_0, V_1 \in \text{St}(s, r)$ . The  $r$  angles between  $V_0, V_1$  are defined by the singular-value decomposition

$$L \cos \Theta R^\dagger \equiv V_1^\dagger V_0 \quad (1)$$

where  $L, R \in U(r)$ ,  $\cos \Theta$  is a non-negative diagonal matrix, and the  $r$  angles are the diagonal elements of  $\Theta$ . Geometrically, the column vectors of  $V_0 R$  and  $V_1 L$  span the two hyperplanes, respectively, and the angle between the  $i$ th column vector of  $V_0 R$ , denoted as  $R_i$ , and the  $i$ th column vector of  $V_1 L$ , denoted as  $L_i$ , is the  $i$ th diagonal element of  $\Theta$ , denoted as  $\Theta_i$ . If we rotate  $R_i$  towards  $L_i$  by the amount of  $t\Theta_i$  for  $t \in [0, 1]$ , and we collect these rotated vectors for all  $i$ 's to span a new hyperplane as a function of  $t$ , then the resulting hyperplane is the geodesic connecting the two hyperplanes represented by

$V_0$  and  $V_1$ , which can be represented by

$$\begin{aligned} \tilde{V}(t) = & V_0 R \csc \Theta \sin [(1-t)\Theta] R^\dagger \\ & + V_1 L \csc \Theta \sin [t\Theta] R^\dagger \end{aligned} \quad (2)$$

Notice that  $\tilde{V}(t)$  is unique if and only if  $\cos \Theta$  is positive definite. If  $\cos \Theta$ 's diagonal contains zeros, then the two hyperplanes are too far from each other to define a unique geodesic, so Eq. (2) is no longer valid. A special property of  $\tilde{V}(t)$  is that its corresponding Berry connection vanishes, i.e.,

$$\tilde{V}^\dagger(t) \partial_t \tilde{V}(t) = 0 \quad (3)$$

However, one can verify that  $\tilde{V}(0) = V_0$  and  $\tilde{V}(1) = V_1 L R^\dagger \simeq V_1$ , i.e., a gauge transformation is applied at  $t = 1$ . We can "repair" the gauge by adopting another representation of the same geodesic in  $\text{Gr}(s, r)$ , e.g.,  $\tilde{V}(t) \equiv \tilde{V}(t) \exp [t \ln (R L^\dagger)]$ . One can verify that  $\tilde{V}(0) = V_0$  and  $\tilde{V}(1) = V_1$ , however, the Berry connection of this new representation no longer vanishes, i.e.,  $\tilde{V}^\dagger \partial_t \tilde{V} = \ln (R L^\dagger)$ . In the Supplemental Materials [25], we will show that  $\tilde{V}$  can be used to reproduce the existing algorithm for calculating the 1st Chern number in a discrete Brillouin zone [22].

The geodesic in Eq. (2) is a one-dimensional interpolant provided two endpoints  $V_0$  and  $V_1$ . From Eq. (2), we can generate the  $D$ -dimensional interpolant  $\tilde{V}(\mathbf{k})$  that defines the Chern numbers. The grid  $K_0$  divides the parameter space  $K$  into  $N_0^D$   $D$ -dimensional hypercubes, and we use  $C_\kappa$  to denote the hypercube whose vertex closest to the origin is  $\kappa \in K_0$ , i.e., if  $\mathbf{k} \in C_\kappa$  then its components satisfy  $0 \leq k^i - \kappa^i \leq N_0^{-1}$ . To get  $\tilde{V}(\mathbf{k})$ , we recursively define  $V_\kappa^{(0)}(\mathbf{k})$  as follows: Given an integer  $0 < i \leq D$ , for  $\mathbf{k} \in C_\kappa$  that satisfies  $k^j = \kappa^j$  or  $\kappa^j + N_0^{-1}$  for any  $j < i$ ,  $V_\kappa^{(i-1)}(\mathbf{k})$  is defined as the right hand side of Eq. (2) with the following replacement:  $V_0 \rightarrow V_\kappa^{(i)}(P_{\kappa,0}^i(\mathbf{k}))$ ,  $V_1 \rightarrow V_\kappa^{(i)}(P_{\kappa,1}^i(\mathbf{k}))$ , and  $t \rightarrow N_0(k^i - \kappa^i)$  with the initial condition  $V_\kappa^{(D)}(\mathbf{k}) \equiv V(\mathbf{k})$ , where the projection operator  $P_{\kappa,t}^i$  for  $0 \leq t \leq 1$  applied to  $\mathbf{k}$  changes  $k^i$  to  $t N_0^{-1} + \kappa^i$  while it keeps other components of  $\mathbf{k}$  invariant. In these recursive procedures, we assume that at each time we use Eq. (2),  $V_0$  and  $V_1$  are close enough such that  $\tilde{V}(t)$  is unique, which can be achieved with a large enough  $N_0$ . In the Supplemental Material [25], the recursive procedure is explicitly shown for calculating the first Chern number in a two-dimensional parameter space.

$V_\kappa^{(0)}(\mathbf{k})$  is a smooth function with well-defined derivatives in its domain  $C_\kappa$ . We define  $\tilde{V}(\mathbf{k})$  piecewise as  $V_\kappa^{(0)}(\mathbf{k})$ , i.e.,  $\tilde{V}(\mathbf{k}) \equiv V_\kappa^{(0)}(\mathbf{k})$  if  $\mathbf{k} \in C_\kappa$ . This definition is ambiguous (multi-valued) on the boundaries of  $C_\kappa$ , however, this ambiguity will not affect the Chern numbers, because the hyperplane represented by  $\tilde{V}(\mathbf{k})$

is unique, i.e., given  $\kappa_0$  and  $\kappa_1$  such that  $C_{\kappa_0} \cap C_{\kappa_1}$  is non-empty,  $V_{\kappa_0}^{(0)}(\mathbf{k}) \simeq V_{\kappa_1}^{(0)}(\mathbf{k})$  for any  $\mathbf{k} \in C_{\kappa_0} \cap C_{\kappa_1}$ . The proof of this statement is given in the Supplemental Material [25]. As a result,  $\tilde{\rho}(\mathbf{k}) \equiv \tilde{V}(\mathbf{k}) \tilde{V}^\dagger(\mathbf{k})$  is a single-valued, continuous, but not necessarily smooth function for  $\mathbf{k} \in K$ . The lack of smoothness does not affect calculating the Chern numbers as long as we piecewise evaluate the defining integral, i.e.,

$$c_n[\tilde{V}] \equiv \sum_{\kappa} \int_{C_\kappa} \text{ch}_n[V_\kappa^{(0)}(\mathbf{k})] d^{2n}k \quad (4)$$

This statement can be verified by showing that the Chern number defined by Eq. (4) coincides with  $c_n[V(\mathbf{k})]$  given a large enough  $N_0$ . By increasing  $N_0$ , the distance between  $V(\mathbf{k}_1)$  and  $V(\mathbf{k}_2)$  decreases for any  $\mathbf{k}_1, \mathbf{k}_2 \in C_\kappa$ . For a large  $N_0$ , such distances are so small that there exists a unique geodesic, represented by  $v(t, \mathbf{k})$  with  $t \in [0, 1]$ , connecting  $V(\mathbf{k})$  and  $V_\kappa^{(0)}(\mathbf{k})$ , i.e.,  $v(0, \mathbf{k}) \simeq V(\mathbf{k})$  and  $v(1, \mathbf{k}) \simeq V_\kappa^{(0)}(\mathbf{k})$ . Now,  $v(t, \mathbf{k})$  establishes a continuous deformation (homotopy) between  $V(\mathbf{k})$  and  $V_\kappa^{(0)}(\mathbf{k})$ , which guarantees that Eq. (4) equals to  $c_n[V(\mathbf{k})]$ .

In conclusion, given the Hamiltonians  $H(\kappa)$  where  $\kappa$  belong to a finite-size ( $N_0^D$ ) grid in the parameter space  $K$ , we can define and calculate to arbitrary precision the Chern numbers, which coincide with the Chern numbers of the continuous mapping  $H(\mathbf{k})$  with  $\mathbf{k} \in K$ . Our result has two inferences: 1. It provides a highly efficient algorithm to numerically calculate the Chern numbers; 2. For systems with a discrete parameter space, e.g., a finite-size tight-binding model with periodical boundary conditions, our method provides an *ab initio* definition of Chern numbers, which may open up a plethora of new opportunities in topological physics. Topological invariants other than the Chern numbers might have a different classifying space than the Grassmann manifold [26]. For example, if the single-particle Hamiltonian  $h(\mathbf{k})$  is a  $2s \times 2s$  hermitian matrix with chiral symmetry, its corresponding many-particle ground state is no longer described by a matrix  $V(\mathbf{k})$  in the Stiefel manifold, but is described by a unitary matrix  $q(\mathbf{k}) \in U(s)$ , and if  $q(\mathbf{k})$  is regarded as mapping from the parameter space to  $U(s)$ , it can be topologically classified by a winding number [26]. To define and calculate the winding number of the discrete mapping  $q(\kappa)$  where  $\kappa$  belongs to a grid, one should find the geodesic interpolants  $\tilde{q}(\mathbf{k})$  of  $q(\kappa)$ , which can be done following the same procedure as the one for interpolating  $V(\kappa)$  with the only modification that Eq. (2) should be replaced by the equation of geodesics in  $U(s)$ , i.e.,  $q_0, q_1 \in U(s)$  are connected by  $\tilde{q}(t) = q_0 \exp\left(t \ln\left(q_0^\dagger q_1\right)\right)$ .

Finally, we provide additional information on the numerical implementation as well as the benchmark of the algorithm for calculating the Chern numbers. Instead

of direct evaluation of Eq. (4), the algorithm can be further optimized. We assume  $D = 2n$  for simplicity. Direct numerical evaluation of Eq. (4) requires the values  $V_{\kappa}^{(0)}(\mathbf{k})$  for  $\mathbf{k}$  on a grid in  $C_{\kappa}$  consisting of  $O(N_1^D)$  points, where  $N_1$  is the number of different values of  $t$  for which  $\tilde{V}(t)$  in Eq. (2) is evaluated. The larger  $N_1$  is, the better the precision will be. Using the generalized Stokes' theorem, the  $D$ -dimensional "bulk" integral  $\int_{C_{\kappa}} \text{ch}_n[V_{\kappa}^{(0)}(\mathbf{k})] d^D k$  in Eq. (4) can be reduced to a  $(D-1)$ -dimensional "surface" integral, whose integrand is the Chern-Simons form [1, 26], and now only  $O(N_1^{D-1})$  times of evaluation of  $V_{\kappa}^{(0)}(\mathbf{k})$  is required. This is possible because  $V_{\kappa}^{(0)}(\mathbf{k})$  is a smooth function in  $C_{\kappa}$ , even though  $V(\mathbf{k})$  is rarely smooth in numerics. In particular, to calculate the second Chern number  $c_2$  in our benchmark, we rewrite Eq. (4) as

$$c_2[\tilde{V}] \equiv -\frac{1}{8\pi^2} \sum_{\kappa} \int_{\partial C_{\kappa}} \epsilon^{\mu\nu\lambda\delta} \text{tr} \left( \mathcal{A}_{\mu}^{(\kappa)} \partial_{\nu} \mathcal{A}_{\lambda}^{(\kappa)} + \frac{2}{3} \mathcal{A}_{\mu}^{(\kappa)} \mathcal{A}_{\nu}^{(\kappa)} \mathcal{A}_{\lambda}^{(\kappa)} \right) d^3 s_{\delta} \quad (5)$$

where  $\mathcal{A}_{\mu}^{(\kappa)} \equiv (V_{\kappa}^{(0)})^{\dagger} \partial_{\mu} V_{\kappa}^{(0)}$  and  $d^3 s_{\delta}$  is the 3-dimensional "surface" element in the direction  $\delta$ . As a result of Eq. (3),  $\mathcal{A}_1^{(\kappa)} = 0$ , which can provide further simplification of Eq. (5). In the Supplemental Material [25], details of optimization are presented in the Python code for the benchmark of the optimized algorithm, named Itp+CS (Interpolation plus Chern-Simons Forms), and also a code for the algorithm used in [19], named 4DItg (4-dimensional Integration). Both algorithms are applied to calculate the 2nd Chern number of the lattice Dirac model with the Hamiltonian  $H_{\text{Dirac}}(\mathbf{k}) = \mathbf{d}(\mathbf{k}) \cdot \mathbf{\Gamma}$  where  $\mathbf{d}(\mathbf{k})$  has 5 components  $d^0 = m + \sum_{i=1}^4 \cos 2\pi k_i$  and  $d^i = \sin 2\pi k_i$  for  $i = 1, 2, 3, 4$ , and  $\mathbf{\Gamma}$  are Dirac matrices represented by products of Pauli matrices

$$\mathbf{\Gamma} = (\sigma_x \otimes \mathbb{1}, \sigma_y \otimes \mathbb{1}, \sigma_y \otimes \sigma_x, \sigma_y \otimes \sigma_y, \sigma_z \otimes \sigma_z)$$

The parameter  $m$  determines the topological phase and there is a topological phase boundary at  $m = 0$ . In the benchmark, Itp+CS diagonalizes  $H_{\text{Dirac}}(\mathbf{k})$  on the lattice  $K_0$  with a fixed  $N_0 = 4$ , and then interpolates the output with a varying  $N_1$  to get  $V_{\kappa}^{(0)}(\mathbf{k})$  for integrating the Chern-Simons form. Meanwhile, 4DItg diagonalizes  $H_{\text{Dirac}}(\mathbf{k})$  on the lattice  $K_0$  but with a varying  $N_0$ , and we denote this varying  $N_0$  as  $N_2$  for distinguishing it from the fixed one used in Itp+CS. By setting  $N_2 = N_0 N_1$ , we plot in Fig. 1(a) the relative error of the 2nd Chern number calculated by the two algorithms for different values of  $m$  that approach the topological phase boundary  $m = 0$ , and in Fig. 1(b) the typical time cost of the two algorithms. The results show that Itp+CS always outperforms 4DItg in both precision and speed. Especially, when it is close to a phase transition, i.e.,  $m = 0.1$

or 0.01, 4DItg fails to converge while Itp+CS provides almost the same level of precision as it does when  $m = 1$ .

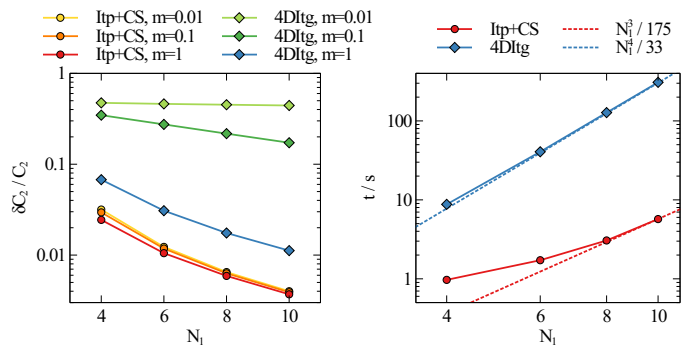


FIG. 1. (Color online) We calculate the second Chern number of the Dirac lattice model using both our new algorithm Itp+CS and the previously established one, 4DItg [19], with varying grid density and compare (a) the relative error and (b) the time cost.

This work was supported by the Deutsche Forschungsgemeinschaft (DFG, German Research Foundation) under Project No. 277974659 via Research Unit FOR 2414. The authors gratefully acknowledge the Gauss Centre for Supercomputing e.V. (www.gauss-centre.eu) for funding this project by providing computing time through the John von Neumann Institute for Computing (NIC) on the GCS Supercomputer JUWELS at Jülich Supercomputing Centre (JSC). Calculations for this research were also performed on the Goethe-NHR high performance computing cluster. The cluster is managed by the Center for Scientific Computing (CSC) of the Goethe University Frankfurt.

- 
- [1] M. Nakahara, *Geometry, topology and physics* (CRC press, 2018).
  - [2] M. Z. Hasan and C. L. Kane, *Rev. Mod. Phys.* **82**, 3045 (2010).
  - [3] X.-L. Qi and S.-C. Zhang, *Rev. Mod. Phys.* **83**, 1057 (2011).
  - [4] A. Bansil, H. Lin, and T. Das, *Rev. Mod. Phys.* **88**, 021004 (2016).
  - [5] C. Nayak, S. H. Simon, A. Stern, M. Freedman, and S. Das Sarma, *Rev. Mod. Phys.* **80**, 1083 (2008).
  - [6] N. R. Cooper, J. Dalibard, and I. B. Spielman, *Rev. Mod. Phys.* **91**, 015005 (2019).
  - [7] X.-G. Wen, *Rev. Mod. Phys.* **89**, 041004 (2017).
  - [8] T. Ozawa, H. M. Price, A. Amo, N. Goldman, M. Hafezi, L. Lu, M. C. Rechtsman, D. Schuster, J. Simon, O. Zeitlinger, and I. Carusotto, *Rev. Mod. Phys.* **91**, 015006 (2019).
  - [9] E. J. Bergholtz, J. C. Budich, and F. K. Kunst, *Rev. Mod. Phys.* **93**, 015005 (2021).
  - [10] T. Ozawa and H. M. Price, *Nat. Rev. Phys.* **1**, 349 (2019).
  - [11] D. J. Thouless, M. Kohmoto, M. P. Nightingale, and M. den Nijs, *Phys. Rev. Lett.* **49**, 405 (1982).



- [12] M. Kohmoto, *Ann. Phys.* **160**, 343 (1985).  
 [13] Y. Hatsugai, *Phys. Rev. Lett.* **71**, 3697 (1993).  
 [14] X.-L. Qi, T. L. Hughes, and S.-C. Zhang, *Phys. Rev. B* **78**, 195424 (2008).  
 [15] C. H. Lee, Y. Wang, Y. Chen, and X. Zhang, *Phys. Rev. B* **98**, 094434 (2018).  
 [16] Y. E. Kraus, Z. Ringel, and O. Zeitlinger, *Phys. Rev. Lett.* **111**, 226401 (2013).  
 [17] M. Koshino and H. Oka, *Phys. Rev. Res.* **4**, 013028 (2022).  
 [18] K. Yamamoto and M. Koshino, *Phys. Rev. B* **105**, 115410 (2022).  
 [19] M. Mochol-Grzelak, A. Dauphin, A. Celi, and M. Lewenstein, *Quan. Sci. Tech.* **4**, 014009 (2018).  
 [20] Z. Wang and S.-C. Zhang, *Phys. Rev. X* **2**, 031008 (2012).  
 [21] Z. Wang and B. Yan, *J. Phys. Condens. Matter.* **25**, 155601 (2013).  
 [22] T. Fukui, Y. Hatsugai, and H. Suzuki, *J. Phys. Soc. Japan.* **74**, 1674 (2005), <https://doi.org/10.1143/JPSJ.74.1674>.  
 [23] Y.-C. Wong, *Proc. Natl. Acad. Sci. U.S.A.* **57**, 589 (1967).  
 [24] S. Berceanu, *Bull. Belg. Math. Soc. - Simon Stevin* **4**, 205 (1997).  
 [25] The Supplemental Material includes: i. The explicit procedure of a two-dimensional interpolation that reproduces the known algorithm for the first Chern number; ii. The proof of the uniqueness of the interpolant hyperplane; iii. The Python code that illustrates the algorithm for the second Chern number and compares its performance against a previously established method..  
 [26] C.-K. Chiu, J. C. Y. Teo, A. P. Schnyder, and S. Ryu, *Rev. Mod. Phys.* **88**, 035005 (2016).

---

## Supplemental Material - Getting topological invariants from snapshots: a protocol for defining and calculating topological invariants of systems with discrete parameter space

### THE ALGORITHM FOR THE 1ST CHERN NUMBER

We show that the algorithm in [22] for calculating  $c_1$  can be reproduced from the geodesic interpolant  $\bar{V}(t) \equiv \tilde{V}(t) \exp[t \ln(RL^\dagger)]$  where the quantities on the r.h.s. of this equation are defined by Eq. (1-2) in the main text. Consider a two-dimensional ( $D = 2$ ) parameter space  $K$ . Knowing  $V(\kappa)$  for  $\kappa$  belonging to the lattice  $K_0$  in  $K$ , the two-dimensional interpolant  $\tilde{V}(\mathbf{k})$  is obtained in the same way as  $V(\mathbf{k})$ , with the exception that at each time Eq. (2) is used, we apply the additional gauge transformation  $\exp[t \ln(RL^\dagger)]$  to change  $\tilde{V}(t)$  into  $\bar{V}(t)$ .

Let us illustrate these procedures in detail: Denote any  $\kappa \in K_0$  by two integers  $i_1, i_2$  such that  $\kappa = (i_1/N_0, i_2/N_0)$ . In the hypercube  $C_\kappa$ , first we have  $V_\kappa^{(2)}(\mathbf{k}) = V(\mathbf{k})$ , where  $\mathbf{k}$  can only be one of the vertices of  $C(\kappa)$ , i.e.,  $(i_1, i_2)/N_0$ ,  $(i_1 + 1, i_2)/N_0$ ,  $(i_1, i_2 + 1)/N_0$ , or  $(i_1 + 1, i_2 + 1)/N_0$ . Next, we interpolate  $V_\kappa^{(2)}(\mathbf{k})$  along the 2nd dimension to get  $V_\kappa^{(1)}(\mathbf{k})$ .  $V_\kappa^{(1)}(\mathbf{k})$  has two disconnected domains  $k^1 = i_1/N_0$  or  $(i_1 + 1)/N_0$  and its expression is

$$\begin{aligned} V_\kappa^{(1)}(k^1, k^2) &= V_\kappa^{(2)}(k^1, i_2/N_0) R^{(2)} \csc \Theta^{(2)} \sin \left[ (1 - (N_0 k^2 - i_2)) \Theta^{(2)} \right] R^{(2)\dagger} \\ &\quad + V_\kappa^{(2)}(k^1, (i_2 + 1)/N_0) L^{(2)} \csc \Theta^{(2)} \sin \left[ (N_0 k^2 - i_2) \Theta^{(2)} \right] R^{(2)\dagger} \\ &= \bar{V}_\kappa^{(1)}(k^1, k^2) \exp \left[ - (N_0 k^2 - i_2) \ln \left( R^{(2)} L^{(2)\dagger} \right) \right] \end{aligned} \quad (S1)$$

with

$$L^{(2)} \csc \Theta^{(2)} R^{(2)\dagger} \equiv \left[ V_\kappa^{(2)}(k^1, (i_2 + 1)/N_0) \right]^\dagger V_\kappa^{(2)}(k^1, i_2/N_0) \quad (S2)$$

Notice that  $L^{(2)}$ ,  $R^{(2)}$  and  $\csc \Theta^{(2)}$  are functions of  $k^1$ , and we have applied the gauge transformation, in contrast to the main text. Then we interpolate  $\bar{V}_\kappa^{(1)}(k^1, k^2)$  (in the main text  $V_\kappa^{(1)}(k^1, k^2)$ ) to get  $\bar{V}_\kappa^{(0)}(k^1, k^2)$  (in the main text  $V_\kappa^{(0)}(k^1, k^2)$ ), whose domain is  $C_\kappa$

$$\begin{aligned} &\bar{V}_\kappa^{(0)}(k^1, k^2) \exp \left[ - (N_0 k^1 - i_1) \ln \left( R^{(1)} L^{(1)\dagger} \right) \right] \\ &= \bar{V}_\kappa^{(1)}(i_1/N_0, k^2) R^{(1)} \csc \Theta^{(1)} \sin \left[ (1 - (N_0 k^1 - i_1)) \Theta^{(1)} \right] R^{(1)\dagger} \\ &\quad + \bar{V}_\kappa^{(1)}((i_1 + 1)/N_0, k^2) L^{(1)} \csc \Theta^{(1)} \sin \left[ (N_0 k^1 - i_1) \Theta^{(1)} \right] R^{(1)\dagger} \end{aligned} \quad (S3)$$

with

$$L^{(1)} \csc \Theta^{(1)} R^{(1)\dagger} = \left[ \bar{V}_\kappa^{(1)}((i_1 + 1)/N_0, k^2) \right]^\dagger \bar{V}_\kappa^{(1)}(i_1/N_0, k^2) \quad (S4)$$

Notice that  $L^{(1)}$ ,  $R^{(1)}$  and  $\text{csc } \Theta^{(1)}$  are functions of  $k^2$ . We define  $\bar{V}(\mathbf{k})$  piecewise as  $\bar{V}_{\kappa}^{(0)}(\mathbf{k})$ , i.e.,  $\bar{V}(\mathbf{k}) \equiv \bar{V}_{\kappa}^{(0)}(\mathbf{k})$  if  $\mathbf{k} \in C_{\kappa}$ . This definition is not ambiguous because  $\bar{V}(t)$ , unlike  $\tilde{V}(t)$ , conserves the gauge convention, i.e.,  $\bar{V}(0) = V_0$  and  $\bar{V}(1) = V_1$ , see the discussion in the main text after Eq. (2). Nevertheless,  $\bar{V}(\mathbf{k})$  and  $\tilde{V}(\mathbf{k})$  provide the *same* geodesic interpolant because  $\bar{V}(\mathbf{k}) \simeq \tilde{V}(\mathbf{k})$  for all  $\mathbf{k}$ .

The 1st Chern number is given by

$$\begin{aligned} c_1[\bar{V}] &\equiv \sum_{\kappa} \int_{C_{\kappa}} \frac{i}{2\pi} \epsilon^{\mu\nu} \text{tr}(\mathcal{F}_{\mu\nu}) d^2k \\ &= \sum_{\kappa} \oint_{\partial C_{\kappa}} \frac{i}{2\pi} \text{tr}(\mathcal{A}_{\mu}) dk^{\mu} \\ &= \sum_{\kappa} \oint_{\partial C_{\kappa}} \frac{i}{2\pi} \text{tr}(\bar{V}^{\dagger} \partial_{\mu} \bar{V}) dk^{\mu} \end{aligned} \quad (\text{S5})$$

where in the 2nd line we have used Stokes' theorem to cast the two-dimensional integral over  $C_{\kappa}$  into a contour integral along the boundary of  $C_{\kappa}$ , denoted as  $\partial C_{\kappa}$ .  $\partial C_{\kappa}$  has four segments that contribute to the integral in the same manner. For example, consider the segment linking  $(i_1, i_2)/N_0$  to  $(i_1 + 1, i_2)/N_0$ . The contour integral on this segment becomes

$$\begin{aligned} &\int_{i_1/N_0}^{(i_1+1)/N_0} \frac{i}{2\pi} \text{tr}(\bar{V}^{\dagger}(k^1, i_2/N_0) \partial_{\mu} \bar{V}(k^1, i_2/N_0)) dk^1 \\ &= \frac{i}{2\pi} \text{tr} \ln(R^{(1)} L^{(1)\dagger}) \\ &= \frac{i}{2\pi} \ln \det(R^{(1)} L^{(1)\dagger}) \\ &= \frac{i}{2\pi} \ln \frac{\det(R^{(1)} \cos \Theta^{(1)} L^{(1)\dagger})}{\det \cos \Theta} \\ &= \frac{i}{2\pi} \ln \frac{\det(V^{\dagger}((i_1+1)/N_0, i_2/N_0) V((i_1+1)/N_0, i_2/N_0))}{|\det(V^{\dagger}((i_1+1)/N_0, i_2/N_0) V((i_1+1)/N_0, i_2/N_0))|} \end{aligned} \quad (\text{S6})$$

which coincides with Eq. (16) in [22]. In this way, our approach provides an alternative derivation of the algorithm in [22] that can be generalized to other topological invariants.

### PROOF OF THE UNIQUENESS OF $\tilde{\rho}(\mathbf{k})$

Given  $\kappa_0, \kappa_1 \in K_0$  such that  $C_{\kappa_0} \cap C_{\kappa_1}$  is non-empty, we are going to show  $V_{\kappa_0}^{(0)}(\mathbf{k}) \simeq V_{\kappa_1}^{(0)}(\mathbf{k})$  for any  $\mathbf{k} \in C_{\kappa_0} \cap C_{\kappa_1}$  by deduction.

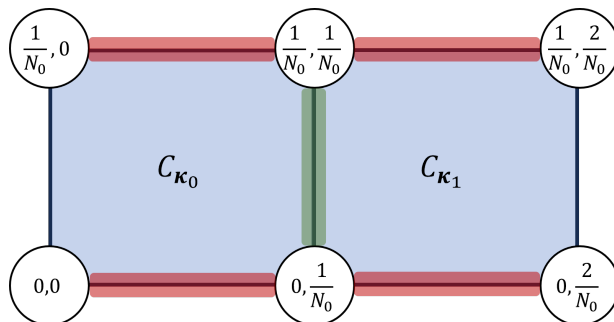


FIG. S1. (Color online) A 2D grid to be interpolated

First, we illustrate the idea of the proof for the case  $D = 2$ . In Fig. S1, we suppose  $C_{\kappa_0}$  and  $C_{\kappa_1}$  are adjacent squares that share an edge.  $V_{\kappa_0}^{(2)}(\mathbf{k})$  and  $V_{\kappa_1}^{(2)}(\mathbf{k})$  are known for  $\mathbf{k}$  at the vertices and their values are simply  $V(\mathbf{k})$ .  $V_{\kappa_0}^{(1)}(\mathbf{k})$  and  $V_{\kappa_1}^{(1)}(\mathbf{k})$  are obtained as interpolants on the red edges of the squares. In particular,

$V_{\kappa_0}^{(1)}(0, 1/N_0) \simeq V_{\kappa_0}^{(2)}(0, 1/N_0) = V_{\kappa_1}^{(2)}(0, 1/N_0) = V_{\kappa_1}^{(1)}(0, 1/N_0)$ , so  $V_{\kappa_0}^{(1)}(0, 1/N_0) \simeq V_{\kappa_1}^{(1)}(0, 1/N_0)$ . For the same reason,  $V_{\kappa_0}^{(1)}(1/N_0, 1/N_0) \simeq V_{\kappa_1}^{(1)}(1/N_0, 1/N_0)$ . In the next step of interpolation, on the green edge,  $V_{\kappa_i}^{(0)}(\mathbf{k})$  is determined by  $V_{\kappa_i}^{(1)}(0, 1/N_0)$  and  $V_{\kappa_i}^{(1)}(1/N_0, 1/N_0)$  for  $i = 0$  or  $1$ . Then  $V_{\kappa_0}^{(0)}(\mathbf{k}) \simeq V_{\kappa_1}^{(0)}(\mathbf{k})$  on the green edge follows from the uniqueness of the geodesic, because they connect the same set of two hyperplanes.

Now consider the general case. Define  $\xi \equiv \kappa_1 - \kappa_0$ . Because  $C_{\kappa_0} \cap C_{\kappa_1}$  is non-empty,  $\xi^i$  can only be  $0$  or  $\pm N_0^{-1}$ . We denote the intersection of the domains of  $V_{\kappa_0}^{(i)}(\mathbf{k})$  and  $V_{\kappa_1}^{(i)}(\mathbf{k})$  as  $I^{(i)}$ . First, by definition we have  $V_{\kappa_0}^{(D)}(\mathbf{k}) = V_{\kappa_1}^{(D)}(\mathbf{k}) = V(\mathbf{k})$  for  $\mathbf{k} \in I^{(D)}$ . Then, suppose  $V_{\kappa_0}^{(i)}(\mathbf{k}) \simeq V_{\kappa_1}^{(i)}(\mathbf{k})$  for  $\mathbf{k} \in I^{(i)}$ . If  $\xi^i = N_0^{-1}$  (or  $-N_0^{-1}$ ), we have  $k^i = \kappa^1$  (or  $\kappa^0$ ) for  $\mathbf{k} \in I^{(i-1)}$ , in other words,  $\mathbf{k} = P_{\kappa_1,0}^i(\mathbf{k}) = P_{\kappa_0,1}^i(\mathbf{k})$  (or  $\mathbf{k} = P_{\kappa_0,0}^i(\mathbf{k}) = P_{\kappa_1,1}^i(\mathbf{k})$ ). As a result,  $V_{\kappa_0}^{(i-1)}(\mathbf{k}) \simeq V_{\kappa_0}^{(i)}(\mathbf{k})$  and  $V_{\kappa_1}^{(i-1)}(\mathbf{k}) \simeq V_{\kappa_1}^{(i)}(\mathbf{k})$ , therefore  $V_{\kappa_0}^{(i-1)}(\mathbf{k}) \simeq V_{\kappa_1}^{(i-1)}(\mathbf{k})$ . If  $\xi^i = 0$ , we have  $P_{\kappa_1,0}^i(\mathbf{k}) = P_{\kappa_0,0}^i(\mathbf{k})$  and  $P_{\kappa_1,1}^i(\mathbf{k}) = P_{\kappa_0,1}^i(\mathbf{k})$  for  $\mathbf{k} \in I^{(i-1)}$ , so  $V_{\kappa_1}^{(i)}(P_{\kappa_1,0}^i(\mathbf{k})) \simeq V_{\kappa_0}^{(i)}(P_{\kappa_0,0}^i(\mathbf{k}))$  and  $V_{\kappa_1}^{(i)}(P_{\kappa_1,1}^i(\mathbf{k})) \simeq V_{\kappa_0}^{(i)}(P_{\kappa_0,1}^i(\mathbf{k}))$ . Then from Eq. (2) we know  $V_{\kappa_0}^{(i-1)}(\mathbf{k}) \simeq V_{\kappa_1}^{(i-1)}(\mathbf{k})$ . So we have proved that  $V_{\kappa_0}^{(0)}(\mathbf{k}) \simeq V_{\kappa_1}^{(0)}(\mathbf{k})$  for  $\mathbf{k} \in I^{(0)}$  and the piecewise function  $\tilde{V}(\mathbf{k})$  defines a unique interpolant hyperplane  $\tilde{\rho}(\mathbf{k}) \equiv \tilde{V}(\mathbf{k})\tilde{V}^\dagger(\mathbf{k})$  for  $\mathbf{k} \in K$ .

### PYTHON CODE FOR THE BENCHMARK

```
# -*- coding: utf-8 -*-
"""
```

```
Benchmark the two algorithms Itp+CS3 and 4DItg that
calculate the 2nd Chern numbers of the
Dirac lattice model.
```

```
@author: Youjiang Xu
"""
```

```
from multiprocessing import Pool
from time import perf_counter
```

```
import numpy as np
import scipy.linalg as sla
```

```
PI2 = 2 * np.pi
PI22 = PI2 * PI2
```

```
#####
#Pauli matrices and Dirac matrices
sigma = [
    np.eye(2, dtype=complex),
    np.array([[0., 1.],[1., 0.]], dtype=complex),
    np.array([[0., -1j],[1j, 0.]], dtype=complex),
    np.array([[1., 0.],[0., -1.]], dtype=complex)
]
Gamma = [
    np.kron(sigma[3], sigma[0]),
    np.kron(sigma[1], sigma[1]),
    np.kron(sigma[1], sigma[2]),
    np.kron(sigma[1], sigma[3]),
    np.kron(sigma[2], sigma[0])
]
```

```

#####
#Some simple routines that will be used in the later part of the code
def uni(U):
    L, _, RH = sla.svd(U, full_matrices=False)
    return L @ RH

def mdot(V0, V1):
    return V0.T.conj() @ V1

def mdotR(V0, V1):
    return V0 @ V1.T.conj()

def logm_norm(A):
    w, v = sla.eig(A)
    return (v* (np.log(w)[None,:])) @ v.T.conj()

def logm_norm_batch(A):
    for ii in np.ndindex(A.shape[:-2]):
        A[ii] = logm_norm(A[ii])

def add_int2tuple(t : tuple, i : int, axis : int = 0):
    return t[:axis] + (t[axis]+i,) + t[axis+1:]

def measureFuncCall(func, *args):
    """
    Measure the time cost of the function call func(args)
    """
    start = perf_counter()
    ret = func(*args)
    end = perf_counter()
    print(f'{func.__name__} took {end - start:.4f} seconds')
    return ret

#####
#The function that gives the 2 lower energy states of the lattice Dirac model
def DiracLowerBands(m : float, c :float, k : np.ndarray):
    ds = np.empty((5,), dtype=float)
    ds[0] = m + c * np.sum(np.cos(PI2 * k))
    ds[1:] = np.sin(PI2 * k)
    H = sum(ds[i] * Gamma[i] for i in range(5))
    _, vH = sla.eigh(H)
    return vH[:, :2]

#####
#The functions in this part implements the new algorithm Itp+CS
def interpV1(V: np.ndarray, len_grid: int = 8, axis: int = -3):
    """
    Interpolate 'V' along a single axis specified by 'axis'.

    Parameters
    -----
    V ((N1, ..., ND, dV, nV) complex ndarray) :

```



```

    'V[i1,...,iD]' represents 'nV' orthonormal vectors of dimension 'dV'
len_grid (int) :
    V is interpolated at the points specified by
    'grid = np.linspace(0., 1., len_grid, endpoint=False)'.
    'V[i1..., i_axis:i_axis+2,...iD]' determines the interpolant
    'IV[i1..., i_axis*len_grid:(i_axis+1)*len_grid,...iD]'
axis (int) :
    Indicates along which axis 'V' is interpolated

```

#### Returns

```

IV ((N1, ..., Naxis * lg + 1, ..., ND, DH, numV) complex ndarray) :
    Interpolant of 'V'

```

```

"""

```

```

grid = np.linspace(0., 1., len_grid, endpoint=False)

```

```

IV = np.empty(
    V.shape[:axis] + ((V.shape[axis] - 1)*len_grid + 1,) + V.shape[axis+1:],
    dtype=complex
)

```

```

for ii in np.ndindex(V.shape[:axis]):
    for kk in np.ndindex(V.shape[axis+1:-2]):
        IV[ii][0][kk] = V[ii][0][kk]
        for j in range(V.shape[axis]-1):
            V0 = IV[ii][j*len_grid][kk]
            V1 = V[ii][j+1][kk]
            L, S, RH = sla.svd(mdot(V1, V0))
            U1 = V1 @ L
            if (len_grid > 1):
                Theta = np.arccos(np.clip(S, None, 1.))
                csc = 1. / np.sin(Theta)
                U0 = mdotR(V0, RH)
                IV[ii + (slice(j*len_grid+1,(j+1)*len_grid),) + kk] = \
                    np.tensordot(
                        (U0[None, :, :] * (csc[None, :])
                         * np.sin(np.outer((1. - grid[1:]), Theta))[:, None, :])
                        + U1[None, :, :] * (csc[None, :])
                         * np.sin(np.outer((grid[1:]), Theta))[:, None, :]),
                        RH,
                        1
                    )
            IV[ii][((j+1)*len_grid)][kk] = U1 @ RH
return IV

```

```

def interpVD(V: np.ndarray, len_grid_arr: np.ndarray):

```

```

"""

```

```

Do the 1D interpolation 'interpV1' along each axis of 'V'

```

#### Parameters

```

V ((N1, ..., ND, dV, nV) complex ndarray) :
    'V[i1,...,iD]' represents 'nV' orthonormal vectors of dimension 'dV'
len_grid_arr (int ndarray) :

```

'V' is interpolated along ith direction with the number of grid points given by 'len\_grid\_arr[i]'.  
See 'interpV1'.

Returns

IV (... , Ni \* len\_grid\_arr[i] + 1, ... , dV, nV) complex ndarray :  
Interpolant of V.

"""

IV = V

D = V.ndim - 2

for axis in reversed(range(D)):

    IV = interpV1(IV, len\_grid\_arr[axis], axis)

return IV

def calcA(V : np.ndarray, D : int = 3):

"""

Calculate the Berry connection A

"""

A = np.zeros((D,) + V.shape[:D] + (V.shape[-1,])\*2, dtype=complex)

for axis in range(D):

    shape\_i = add\_int2tuple(V.shape[:D], -1, axis)

    for jj in np.ndindex(shape\_i):

        kk = add\_int2tuple(jj, 1, axis)

        A[axis][jj] = logm\_norm(uni(mdot(V[jj], V[kk])))

return A

def calcCS3(A):

CS3\_shape = np.array(A.shape[1:4]) - np.ones(3, dtype=int)

CS3 = np.empty(CS3\_shape, dtype=float)

for ii in np.ndindex(CS3.shape):

    ii0 = add\_int2tuple(ii, 1, 0)

    ii1 = add\_int2tuple(ii, 1, 1)

    ii2 = add\_int2tuple(ii, 1, 2)

    ii01 = add\_int2tuple(ii0, 1, 1)

    ii02 = add\_int2tuple(ii0, 1, 2)

    ii12 = add\_int2tuple(ii1, 1, 2)

    A0 = A[0][ii] + A[0][ii1] + A[0][ii2] + A[0][ii12]

    A1 = A[1][ii] + A[1][ii0] + A[1][ii2] + A[1][ii02]

    A2 = A[2][ii] + A[2][ii0] + A[2][ii1] + A[2][ii01]

    p1A0 = A[0][ii1] - A[0][ii] + A[0][ii12] - A[0][ii2]

    p2A0 = A[0][ii2] - A[0][ii] + A[0][ii12] - A[0][ii1]

    p0A1 = A[1][ii0] - A[1][ii] + A[1][ii02] - A[1][ii2]

    p2A1 = A[1][ii2] - A[1][ii] + A[1][ii02] - A[1][ii0]

    p0A2 = A[2][ii0] - A[2][ii] + A[2][ii01] - A[2][ii1]

    p1A2 = A[2][ii1] - A[2][ii] + A[2][ii01] - A[2][ii0]

    CS3[ii] = np.trace(  
        A0@(p1A2 - p2A1) + A1@(p2A0 - p0A2) + A2@(p0A1 - p1A0)  
    ).real \

        + np.trace(A0 @ A1 @ A2).real / 2.

return CS3 / (PI22 \* 16.)

def calcCS3\_A0is0(A):

CS3\_shape = np.array(A.shape[1:4]) - np.ones(3, dtype=int)

```

CS3 = np.empty(CS3_shape, dtype=float)
for ii in np.ndindex(CS3.shape):
    ii0 = add_int2tuple(ii, 1, 0)
    ii1 = add_int2tuple(ii, 1, 1)
    ii2 = add_int2tuple(ii, 1, 2)
    ii01 = add_int2tuple(ii0, 1, 1)
    ii02 = add_int2tuple(ii0, 1, 2)
    A1 = A[1][ii] + A[1][ii0] + A[1][ii2] + A[1][ii02]
    A2 = A[2][ii] + A[2][ii0] + A[2][ii1] + A[2][ii01]
    p0A1 = A[1][ii0] - A[1][ii] + A[1][ii02] - A[1][ii2]
    p0A2 = A[2][ii0] - A[2][ii] + A[2][ii01] - A[2][ii1]
    CS3[ii] = np.trace(A2 @ p0A1 - A1 @ p0A2).real
return CS3 / (PI22 * 16.)

```

```

def intCS3_block(
    Vblock : np.ndarray,
    len_grid : int = 8,
    IV0 : np.ndarray = None, IV1 : np.ndarray = None,
    flag_greedy : bool = True):
    """Integrate the Chern–Simons form in the boundary of a 4D cube
    Args:
        Vblock ((2,2,2,2,dV,nV) complex ndarray):
            ‘V[i1,...,iD]’ represents ‘nV’ orthonormal vectors of dimension ‘dV’

        len_grid (int, optional):
            The length of the grid fed to ‘interp1D’. Defaults to 8.

        IV0: 3D interpolants of V[0]

        IV1: 3D interpolants of V[1]

        flag_greedy (bool) : if ‘False’, simply integrate the Chern–Simons form;
            if ‘True’, use the faster method that
            for some parts of the boundaries
            calculates the sum of the two integrals contributed by
            two adjacent 4D cubes, therefore the result is meaningful
            only when the results from all 4D cubes are summed up

    Returns:
        float : The integrated Chern–Simons form.
    """
    dim = 3

    grid3D = np.array((len_grid,)*3)
    if IV0 is None:
        IV0 = interpVD(Vblock[0], grid3D)
    if IV1 is None:
        IV1 = interpVD(Vblock[1], grid3D)
    IV2 = np.empty_like(IV0)
    for ii in np.ndindex(IV0.shape[:-2]):
        IV2[ii] = IV1[ii] @ uni(mdot(IV1[ii], IV0[ii]))

    A0 = calcA(IV0)
    A2 = calcA(IV2)

    ret = np.sum(calcCS3(A2) - calcCS3_A0is0(A0))

```

```

if flag_greedy:
    coef = 1./(PI22 * 8.)
    for i in range(dim):
        iv = np.take(IV0, -1, i)
        ivg = interpVD(Vblock[0][(slice(None),)*i + (-1,)], (len_grid,)*2)
        g = np.einsum('ijkl,ijkm->ijlm', iv.conj(), ivg)
        dgg = np.zeros((2,)+g.shape, dtype=complex)
        dgg[0, :-1] = np.einsum('ijkl,ijml->ijkm', g[1:], g[:-1].conj())
        logm_norm_batch(dgg[0, :-1])
        dgg[1, :, :-1] = np.einsum('ijkl,ijml->ijkm', g[:, 1:], g[:, :-1].conj())
        logm_norm_batch(dgg[1, :, :-1])

    diff_a = np.delete(A0[(slice(None),)*(i+1) + (-1,)], i, 0) \
        - np.delete(A2[(slice(None),)*(i+1) + (-1,)], i, 0)
    ret += coef * sum(
        (
            np.trace(
                (dgg[0][ii] + dgg[0][add_int2tuple(ii, 1, 1)])
                @(diff_a[1][ii] + diff_a[1][add_int2tuple(ii, 1, 0)])
                -(dgg[1][ii] + dgg[1][add_int2tuple(ii, 1, 0)])
                @(diff_a[0][ii] + diff_a[0][add_int2tuple(ii, 1, 1)])
            ).real

            for ii in np.ndindex((dgg.shape[1]-1, dgg.shape[2]-1))
        )
    )
    coef = -coef
else:
    coef = 1.
    for i in range(dim):
        iv = interpV1(
            np.stack((np.take(IV0, (0, -1), i), np.take(IV1, (0, -1), i)), axis=0),
            len_grid, 0)
        ret += coef * np.sum(
            calcCS3_A0is0(calcA(np.take(iv, 0, i+1)))
            - calcCS3_A0is0(calcA(np.take(iv, -1, i+1)))
        )
        coef = -coef

return ret, IV0, IV1

```

```

def intCS3_stack(Vstack : np.ndarray, len_grid : int = 8, flag_greedy : bool = True):
    """Integrate the Chern–Simons form in a stack of 4D cubes

```

Args:

Vstack ((n\_block, 2, 2, 2, dV, nV) complex ndarray):  
 ‘V[i1, ..., iD]’ represents ‘nV’ orthonormal vectors of dimension ‘dV’

len\_grid (int, optional): The length of the grid fed to ‘interp1D’.  
 Defaults to 8.

flag\_greedy (bool) : See ‘intCS3\_block’

Returns:

float : The integrated Chern–Simons form.  
 """

```

n_block = Vstack.shape[0] - 1
ret, IV0, IV1 = intCS3_block(Vstack[0:2], len_grid, flag_greedy=flag_greedy)
for i in range(1, n_block-1):
    tmp, -, IV1 = \
        intCS3_block(Vstack[i:i+2], len_grid, IV1, flag_greedy=flag_greedy)
    ret += tmp
if n_block > 1:
    if flag_greedy:
        tmp, -, - = \
            intCS3_block(Vstack[-2:], len_grid, IV1, IV0, flag_greedy=flag_greedy)
    else:
        tmp, -, - = \
            intCS3_block(Vstack[-2:], len_grid, IV1, flag_greedy=flag_greedy)
    ret += tmp
return ret

```

```

def intCS3(V : np.ndarray, len_grid : int = 8, flag_greedy : bool = True):
    """Integrate the Chern–Simons form in the whole parameter space
    """
    shape_stack = tuple(np.array(V.shape[1:4], dtype=int) - np.ones(3, dtype=int))
    ret = np.empty(shape_stack, dtype=float)
    args = (
        (V[:, ii[0]:ii[0]+2, ii[1]:ii[1]+2, ii[2]:ii[2]+2], len_grid, flag_greedy)
        for ii in np.ndindex(shape_stack)
    )
    with Pool() as p:
        for ii, tmp in zip(np.ndindex(shape_stack), p.starmap(intCS3_stack, args)):
            ret[ii] = tmp
    return np.sum(ret)

```

```

#####
#The three functions in this part are used to calculate the 2nd Chern number
#by the algorithm proposed in
#M Mochol–Grzelak et al 2019 Quantum Sci. Technol. 4 014009
def intF2_A(A : np.ndarray):
    grid = tuple(np.array(A.shape[1:5], dtype=int) - np.ones(4, dtype=int))
    F = np.empty((6,) + A.shape[-2:], dtype=complex)
    components = [(0,1),(0,2),(0,3),(1,2),(1,3),(2,3)]

    ret = 0.
    for jj in np.ndindex(grid):
        kk = [add_int2tuple(jj, 1, i) for i in range(4)]
        for i, c in enumerate(components):
            F[i] = A[c[0]][jj] @ A[c[1]][jj]
            F[i] -= F[i].T.conj()
            F[i] += A[c[1]][kk[c[0]]] - A[c[1]][jj] \
                - A[c[0]][kk[c[1]]] + A[c[0]][jj]
        ret += np.trace(F[0]@F[5] - F[1]@F[4] + F[2]@F[3])
    return ret / PI22

```

```

def calc_F2_U(Ublock : np.ndarray):
    idx_pair = [(0,1),(0,2),(0,3),(1,2),(1,3),(2,3)]
    F = np.empty((6,) + Ublock.shape[-2:], dtype=complex)

```

```

t0 = (0,0,0,0)
for i, ip in enumerate(idx_pair):
    F[i] = Ublock[ip[0]][t0] \
        @ Ublock[ip[1]][add_int2tuple(t0,1,ip[0])] \
        @ sla.inv(Ublock[ip[0]][add_int2tuple(t0,1,ip[1])]) \
        @ sla.inv(Ublock[ip[1]][t0])
    F[i] = sla.logm(F[i])
return np.trace(F[0]@F[5] - F[1]@F[4] + F[2]@F[3]).real

def intF2(V : np.ndarray):
    U = np.zeros((4,) + V.shape[:4] + (V.shape[-1])*2, dtype=complex)
    for i in range(4):
        U_non0_shape = V.shape[:i] + (V.shape[i]-1,) + V.shape[i+1:4]
        for jj in np.ndindex(U_non0_shape):
            U[i][jj] = mdot(V[jj], V[add_int2tuple(jj, 1, i)])

    grid = tuple(np.array(V.shape[:4], dtype=int) - np.ones(4, dtype=int))
    args = [
        U[:, jj[0]:jj[0]+2, jj[1]:jj[1]+2, jj[2]:jj[2]+2, jj[3]:jj[3]+2]
        for jj in np.ndindex(grid)
    ]
    with Pool() as p:
        return sum(p.map(calc_F2_U, args)) / PI22

#####
if __name__ == "__main__":
    def benchmark_4DInt(N, len_grid, m, c):
        N *= len_grid
        V = np.empty((N+1)*4 + (4, 2), dtype=complex)
        args = ((m, c, np.array(ii, dtype=float)/N) for ii in np.ndindex((N,)*4))
        with Pool() as p:
            for ii, ret in zip(np.ndindex((N,)*4), p.starmap(DiracLowerBands, args)):
                V[ii] = ret
        for i in range(4):
            V[(slice(None),)*i + (-1,)] = V[(slice(None),)*i + (0,)]
        rst = intF2(V)
        return rst, rst - round(rst), abs(1 - round(rst)/rst)

    def benchmark_ItpCS(N, len_grid, m, c, flag_greedy : bool = True):
        V = np.empty((N+1)*4 + (4, 2), dtype=complex)
        args = ((m, c, np.array(ii, dtype=float)/N) for ii in np.ndindex((N,)*4))
        with Pool() as p:
            for ii, ret in zip(np.ndindex((N,)*4), p.starmap(DiracLowerBands, args)):
                V[ii] = ret
        for i in range(4):
            V[(slice(None),)*i + (-1,)] = V[(slice(None),)*i + (0,)]
        rst = intCS3(V, len_grid, flag_greedy)
        return rst, rst - round(rst), abs(1 - round(rst)/rst)

N = 4
len_grid_arr = [4, 6, 8, 10]
m_arr = [1.0, 0.1, 0.01, 3.0, 3.9, 3.99]
c = 1.

```



```
for m in m_arr:
    for len_grid in len_grid_arr:
        print(f"m = {m:}, N1 = {len_grid}")
        print(measureFuncCall(benchmark_ItpCS, N, len_grid, m, c, True))
        print(measureFuncCall(benchmark_4DInt, N, len_grid, m, c))
```